Water Research 234 (2023) 119830

Contents lists available at ScienceDirect

Water Research

journal homepage: www.elsevier.com/locate/watres

Enhancing quorum quenching media with 3D robust electrospinning coating: A novel biofouling control strategy for membrane bioreactors

Haoliang Pang [a,b], Jinhui Huang [a,b,*], Xue Li [c], Kaixin Yi [a,b], Suzhou Li [a,b], Zhexi Liu [a,b], Wei Zhang [a,b], Chenyu Zhang [a,b], Si Liu [a,b], Yanling Gu [d]

[a] College of Environmental Science and Engineering, Hunan University, Changsha, Hunan, 410082, China
[b] Key Laboratory of Environmental Biology and Pollution Control, Hunan University, Ministry of Education, Changsha, Hunan, 410082, China
[c] Hunan Key Laboratory of Applied Environmental Photocatalysis, Changsha University, Changsha 410022, China
[d] College of Materials Science and Engineering, Changsha University of Science and Technology, Changsha 410114, China

ARTICLE INFO

Keywords:
Membrane bioreactor
Biofouling
quorum quenching
Electrospun membrane
3D framework
Structure enhancing

ABSTRACT

Bacterial quorum quenching (QQ) is an effective strategy for controlling biofouling in membrane bioreactor (MBR) by interfering the releasing and degradation of signal molecules during quorum sensing (QS) process. However, due to the framework feature of QQ media, the maintenance of QQ activity and the restriction of mass transfer threshold, it has been difficult to design a more stable and better performing structure in a long period of time. In this research, electrospun fiber coated hydrogel QQ beads (QQ-ECHB) were fabricated by using electrospun nanofiber coated hydrogel to strengthen layers of QQ carriers for the first time. The robust porous PVDF 3D nanofiber membrane was coated on the surface of millimeter-scale QQ hydrogel beads. Biocompatible hydrogel entrapping quorum quenching bacteria (sp.BH4) was employed as the core of the QQ-ECHB. In MBR with the addition of QQ-ECHB, the time to reach transmembrane pressure (TMP) of 40 kPa was 4 times longer than conventional MBR. The robust coating and porous microstructure of QQ-ECHB contributed to keeping a lasting QQ activity and stable physical washing effect at a very low dosage (10g beads/5L MBR). Physical stability and environmental-tolerance tests also verified that the carrier can maintain the structural strength and keep the core bacteria stable when suffering long-term cyclic compression and great fluctuations in sewage quality.

1. Introduction

Membrane bioreactor (MBR) where a technology that combines the advantages of activated biological reaction and membrane separation (Judd 2008, Lee et al. 2016a, Min et al. 2022). In the past 30 years, it has developed into a smaller reactor size that can handle larger fluctuations of effluent water and generate high quality reusable water, evolving into a proven technology(Gu et al. 2018a, Ma et al. 2018). Since the presence of MBR technology, the bottleneck of membrane biofouling has been restricting this technology, and it is also motivating the reform and innovation of this technology(Bagheri and Mirbagheri 2018, Drews 2010, Meng et al. 2009). Quorum sensing (QS) was found to be a phenomenon that bacteria regulate their behaviors in groups, such as virulence and biofilm formation, in a cell-density-dependent way using signal molecules(Miller and Bassler 2001, Oh and Lee 2018, Waters and Bassler 2005). Quorum quenching (QQ) is a physicochemical strategy for biofouling control by inhibiting QS behavior(Marx 2014), it decomposes the signal molecule (AHL) in the QS process by specific enzymes to reduce the density of quorum-sensing bacteria, thereby reducing extracellular polymeric substances (EPS) secretion, slowing down the attachment speed of biofilm, and inhibiting the process of membrane biofouling(Wigginton 2009, Yeon et al. 2009a, Yeon et al. 2009b).

Since Kim et al. first applied QS mechanism to control MBR biofouling in 2009(Yeon et al. 2009a), isolated the QQ bacteria *Rhodococcus* sp. BH4 in MBR in 2012 and entrapped in mobile hydrogel porous spherical beads(Kim et al. 2013), a variety of bacterial immobilization modes have been emerged in the last decade, involving cell entrapping beads (CEBs)(Huang et al. 2019b, Lan et al. 2021, Li et al. 2023, Zeng et al. 2018), microbial-vessel(Oh et al. 2012, Won-Suk et al. 2014), sheets(Nahm et al. 2017), rotary microbial carrier frame (RMCF) (Ergön-Can et al. 2017), co-culture immobilized QQ filter membrane

* Corresponding author at: College of Environmental Science and Engineering, Hunan University, Changsha 410082, China.
E-mail address: huangjinhui_59@163.com (J. Huang).

https://doi.org/10.1016/j.watres.2023.119830
Received 11 January 2023; Received in revised form 27 February 2023; Accepted 1 March 2023
Available online 3 March 2023

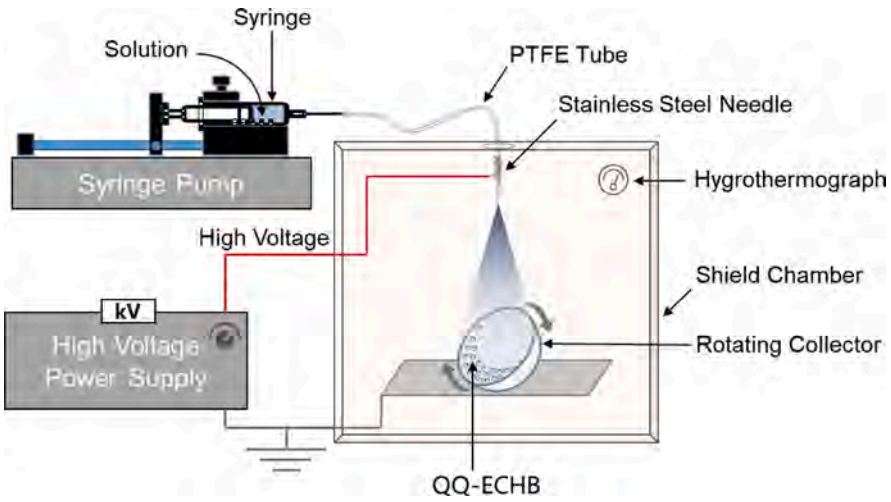

Fig. 1. Electrospinning process of assembly of QQ-ECHB.

and their modified and optimized carriers(Shah et al. 2022). Among a series of spherical, fiber tube, plate-frame structure, and layer by layer (LBL) structures, we found that free-moving millimeter-scale QQ beads are the most reasonable carrier structure for controlling MBR biofouling, for their shape and size can free moving in the aeration environment and scouring the surface of the fiber(Yu et al. 2019), concurrently the entrapped QQ bacteria can inhibit the biofouling of the fiber surface by quorum quenching effect(Kim et al. 2013). However, since the appearance of QQ beads, the structure of beads is usually constructed by gel cross-linking or multi-layer gel cross-linking combined with phase transformation, so in these research, the QQ colony was either exposed to an opening environment connected to the external water environment or barred in a closed system with an outer layer constructed by phase inversion, making potential impacts on the continued quorum quenching or maintaining the integrity and stability of the structure of the beads.

A 3D structure membrane typically has a complex, porous architecture that allows for high permeability and selectivity. The interconnected pores and channels in the membrane provide a large surface area for mass transfer, which can improve the efficiency of separation processes(Li et al. 2020). This research first coupled precise surface electrospinning (ES) technology(Liang et al. 2021, Shin et al. 2018) with the fabrication of QQ beads structure layer, and manufactured a kind of 3D electrospun fibers coated hydrogel QQ beads (QQ-ECHB). ES is commonly employed to produce continuous polymer fibers with diameters in the submicron to micron range through an external electric field applied to a liquid polymer(Huang et al. 2020a, Xue et al. 2019). ES fibers are produced due to uniaxial stretching and elongation of charged elastic polymer jets, formed from viscous solutions or melts, due to electrostatic repulsion of accumulated surface charges and solvent evaporation(Shepa et al. 2021, Shi et al. 2022). Electrospinning has developed into a mature technique for producing high-performance nanofiber membranes and extremely small and nearly mono-disperse particles(Huang et al. 2022, Ramakrishna et al. 2006, Shi et al. 2022). The advanced research of hydrogel coupled nanofiber membranes currently exists in the fabrication of antifouling oil-water separation composite membranes and the application of electroactive hydrogels in bio-nano generators(Cheng et al. 2022, Tan et al. 2022, Tang et al. 2021, Zhu et al. 2021). The development and application of in vivo electrospinning has provided the theoretical foundations and technical support for the fabrication of enhanced coatings on the outside of bacteria-entrapping hydrogels(Diep and Schiffman 2021, Dror et al. 2007, Jayasinghe 2022). Still, the ES coating on the surface of a millimeter scale hydrogel is the first attempt. Fluoropolymer is an ideal candidate for membrane materials for its high energy covalent bond C-F bond and the protective and shielding effect of fluorine atoms on carbon frame, providing excellent physical and chemical stability(Liu et al. 2011, Pang et al. 2021). Polyvinylidene fluoride (PVDF) has been reported to be a semi-crystalline fluorocarbon polymer with excellent chemical resistance, thermal and mechanical properties and have facile and mature membrane-forming process, we chose it as the ideal material for electrospinning(Kang and Cao 2014, Liang et al. 2021, Liu et al. 2011).

Here, a robust 3D porous protective membrane was deposited on the surface of gel beads embedded with *Rhodococcus* sp. BH4 strain by using a self-made ES rotating collector. This outer membrane layer of QQ beads has excellent elasticity and resistance to physical scour and chemical shock, which can protect the core of the beads maintains a complete structure under long-term hydraulic erosion and aeration, and keep the swelling of the gel core under control(Huang et al. 2018). In addition, the porous construction support the core of the beads to exchange materials with the external environment (feeding and metabolism of QQ bacteria). The feasible pore size inhibits the escape of the inner core bacteria, keep the QQ beads continue to exert the quorum quenching effect and stable physical washing.

2. Materials and Methods

2.1. Preparation of QQ-HB

For preparation of QQ-HB, *Rhodococcus* sp. BH4 was used as the QQ bacteria because it has the capacity to continuously produce N-acyl homoserine lactone (AHL) lactonase, which is capable of decomposing a wide variety of signal molecules of AHLs. *Rhodococcus* sp. BH4 were inoculated in Luria–Bertani (LB, AR, SINOPHARM, China) broth at 30 °C for 24h, then transferred the BH4 culture to a centrifuge with the set of 8000g, under the temperature of 4°C, the BH4 grown were resuspended in normal saline after centrifuged for 10min. The preparation of the hydrogel precursor solution is added 10 g polyvinyl alcohol (PVA, 2488, Sinopec, China) powder to 100 mL deionized water and stirred at 85°C for two hours until forming a transparent PVA solution (10%, w/v), then 2g sodium alginate (SA, AR, SINOPHARM, China) was added to the prepared PVA solution, stirring until to form a uniform SA/PVA solution. The 10mL BH4 suspension (200mg/mL of normal saline) was gently mixed with 100 mL of the SA-PVA solution to make a BH4–SA/PVA suspension. The BH4–SA/PVA suspension was dripped into 4% boric acid-1%$CaCl_2$ solution through a nozzle at a rate of 2mL/min, the dripping device include the feeding part, pumping part and cross-linking part. After the initial cross-linking, the QQ-HB were made further dropped into 0.5M sodium sulfate for 8-hour stabilization.

2.2. Pretreatment of QQ-HB

Inspired by cryoprotectants (CPAs) used in the inhibition of the icing of water in biological samples,(Chen et al. 2018, Zhu et al. 2021) glycerol was used to displacing water molecules within the surface of the QQ-HB. Briefly, the original QQ-HB were immersed in a glycerol solution for 20min, to generate the glycerol-based tough hydrogel, we called QQ-HB(g).

2.3. Assembly of QQ-ECHB

The 10 wt% PVDF polymer dope solution was prepared by dissolving PVDF (Mw=400,000, DuPont, USA) in a mixture of DMF (AR, Mclean biochemical technolog, China) and acetone (AR, Mclean biochemical technolog, China)at a volume ratio of 7:3. More specifically, the preparation of QQ-ECHB from QQ-HB(g) is as follows Fig. 1, the QQ-HB(g) were placed in a self-made metal hemispherical rotating collector with a PTFE coating on the inside (Supplementary Movie). Electrospinning of PVDF nanofibers was performed using single nozzle electrospinning system (TL-Pro, Tongli Weina, China) under the following conditions: dope solution feeding rate of 3mL/h, tip to center of rotating collector distance of 10cm, positive voltage of 18kV, and keep the metal shell of the rotating collector grounded in order to promote a stable potential difference between the tip and the collector. Adjust the speed of the rotating collector between 20 to 100 RPM according to the number of QQ-HB(g) to make the beads roll evenly inside the collector. Nanofibers were assembled on the surface of rolling beads under electrostatic attraction and the 3D electrospun nanofibers film covered on the beads as the outer layer of QQ-ECHB.

2.4. Visualization of QQ Bacteria Distribution in Beads

To visualize the active BH4 within the QQ-ECHB, SYTO®9 Green-Fluorescent Nucleic Acid Stains was used to labels all bacteria with intact membranes. Briefly, the cross-section of the beads is cut with a scalpel, gaining in a circular slice about 0.5mm thick, after incubated in SYTO®9 solution (at a final concentration of 30μM) at room temperature in dark for 15 minutes and rinses twice with deionized water, observing directly under the confocal laser-scanning microscope (CLSM, A1+Ti2, Nikon, Japan) at wavelengths of 480nm excitation and 500nm emission(Manteca et al. 2005).

2.5. Evaluation of Mechanical Properties

The compressive property and cyclic compression performance were considered as the mechanical strength of the beads.(Tang et al. 2021) The mechanical compression stress−strain tests of single bead were evaluated by the uniaxial compression test employing an INSTRON materials test system (INSTRON 5982, US) equipped with a 50 N pressure sensor, the force-deformation curve of the bead was drawn from the beginning to the process of complete compression. Considering to evaluate the structural stability of beads under extreme physical scour, the cyclic compression test was employed to describe the change of the compressive properties of beads after multiple high strength compression, the mechanical stability of beads were evaluated by 100 successive loading-unloading cycles.

2.6. Evaluation of the Physical Washing Efficiency

The contribution of QQ-ECHB to the mitigation of membrane biofouling is reflected in the QQ activity and physical washing. The physical washing effect of V-ECHB (Vacant-ECHB, means ECHB not embedding QQ bacteria) and QQ-ECHB were assessed in the batch reactor. 20 of every type of beads were placed in the batch reactor respectively. In each batch reactor, instead of using actual membrane module, there were three PVDF coupons fixed on the internal surface of the container. The batch reactors were operated with or without V-ECHB at an aeration rate of 1.5L/min, and measure the contribution of physical washing in whole mitigation of biofouling properties by comparing with QQ-ECHB result. After 24h aeration, the PVDF coupons were taken out of the batch reactor and stained with 10mL 0.1% (w/v) crystal violet (CV), and the floating color on the coupons was washed carefully with deionized water, then dried for 24 h. Crystal violet on the coupons was dissolved in ethanol by separately immersing the coupons in 10 mL of ethanol solution for 30 min. The concentration of CV in ethanol was measured using a spectrophotometer set at 570 nm. The absorption value of three coupons from one reactor were averaged, and defined as the formed biofilm mass.

2.7. Evaluation of QQ Activity

QQ activity of the beads was analyzed in terms of the degradation rate of commercial AHL, C8-HSL (Sigma-Aldrich, St. Louis, MO), a QS signal molecule. In detail, QQ-media, prepared by fixing their number at 10 pieces, were added to 250μL of 10000μg/mL C8-HSL dissolved in 12.25mL Tris HCl-Trizma (50mM, pH 7) and left to react on an orbital shaker at 130 rpm and 25°C. The C8-HSL concentration was measured using an UHPLC coupled a triple quadrupole mass spectrometer (UHPLC-MS/MS, 1290/6460, Agilent, US) equipped with an electrospray ionization source (ESI) (Agilent, US).(Huang et al. 2020b) The column used was a ZORBAX Eclipse Plus C18 column (2.1 mm × 50 mm with 1.8-μm particle size) equipped with a 0.2-μm in-line filter (Agilent, US). Every single sample need to be desalted and concentrated by solid phase extraction (SPE) before entering UHPLC-MS/MS. The C8-HSL concentration-responses calibration curve is shown in Fig. S1 and detail setup of SPE, UHPLC and MS are shown in Supporting Information Table. S1.

2.8. MBR Setup

Two parallel MBRs (pH = 6.9–7.2) with a working volume of 5L were operated with same aeration intensity of 2L/min. The MLSS and flux of MBRs was 5000 ± 500 mg/L and 24L/m^2/h. Activated sludge was taken from an urban wastewater treatment plant (Changsha, China) and acclimatized until the MBR operating parameters stabilized. The HRT was 18h and there was no backflow and drained activated sludge during the experiment. The composition of the synthetic wastewater in this experiment was as follows (every 50L): glucose, 20g; yeast extract, 0.7g; bactopeptone, 5.75g; $(NH_4)_2SO_4$, 5.25g; KH_2PO_4, 1.0875g; $MgSO_4$, 0.7815g; $CaCl_2$, 0.1225g; $MnSO_4$, 0.09g; and $NaHCO_3$, 12.8g and a little bit of $FeCl_2$ and $CoCl_2$, keeping the COD of the synthetic wastewater is around 400-500mg/L.

The extent of biofouling in the MBRs was reflected by monitor the value of the transmembrane pressure (TMP) during the MBRs operation, and the MBRs were stopped when the TMP reached 40 kPa, the operated time was recorded to evaluate the anti-biofouling performance of the MBRs.(Ouyang et al. 2020) Membranes became fouled during operation were taken out of the reactor and soaked in 1000ppm of NaOCl for 3h to clean and reuse the fouled module.(Lee et al. 2016b) The soluble extracellular products (SMP) and extracellular polymeric substances (EPS) in the mixed liquor were extracted when the TMP of control MBR reached 40 kPa.(Huang et al. 2019a)

2.9. Analytical Methods

To show the efficient transfer of nutrients and signaling molecules between the interlayer of the beads we selected a marker to probe its mass transfer properties in beads with different layered structures. Evaluation of the mass transmissibility were carried out with 20 beads for each type immersed in 50mL 0.5mg/L glucose solution. Experimental samples were withdrawn at interval time, the remaining concentration of the glucose solution was measured by DNS method.

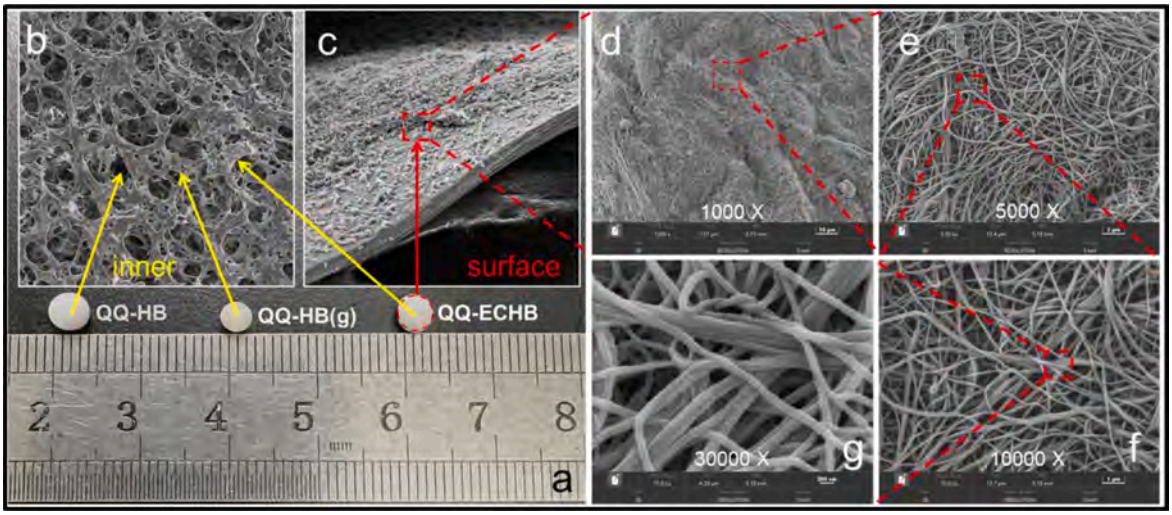

Fig. 2. The macroscopic morphology of the QQ-media (a) and micromorphology under SEM (b, inside the beads; c-g, outer layer).

Investigation of the bacteria leakage of the beads was conducted by culturing the beads in a solid medium for 48h to observe rounding colony growth.

The SMP is obtained by centrifuging the mixed liquor from the MBR at 8000 rpm for 15 minutes and filtering the supernatant through a 0.45μm Millipore filter.(Shi et al. 2017) Then, a thermal extraction method was applied to the extraction of EPS from the remaining sludge pellets.(Yi et al. 2022, Yi et al. 2023) The bound EPS in the mixed liquor can be divided into loosely bound EPS (LB-EPS) and tightly bound EPS (TB-EPS). The polysaccharide and protein concentrations were measured as EPS and SMP concentrations using the phenol-sulfuric acid method and the modified Lowry method respectively.(Gu et al. 2018b, Huang et al. 2019c)

Mixed liquor suspended solids (MLSS) and chemical oxygen demand (COD) were measured according to standard methods.

Meantime, Fourier transform infrared spectroscopy (FTIR) and Thermogravimetric Analysis (TGA) were employed to identify the functional group and compositions of the V-ECHB.

To observe the microstructure of the layer of the beads, the core-shell beads were cut into half and treated by freeze-dried and coated with a gold layer, scanning electron microscopy (SEM) was used to characterize the surface and cross-sectional structure of the beads.

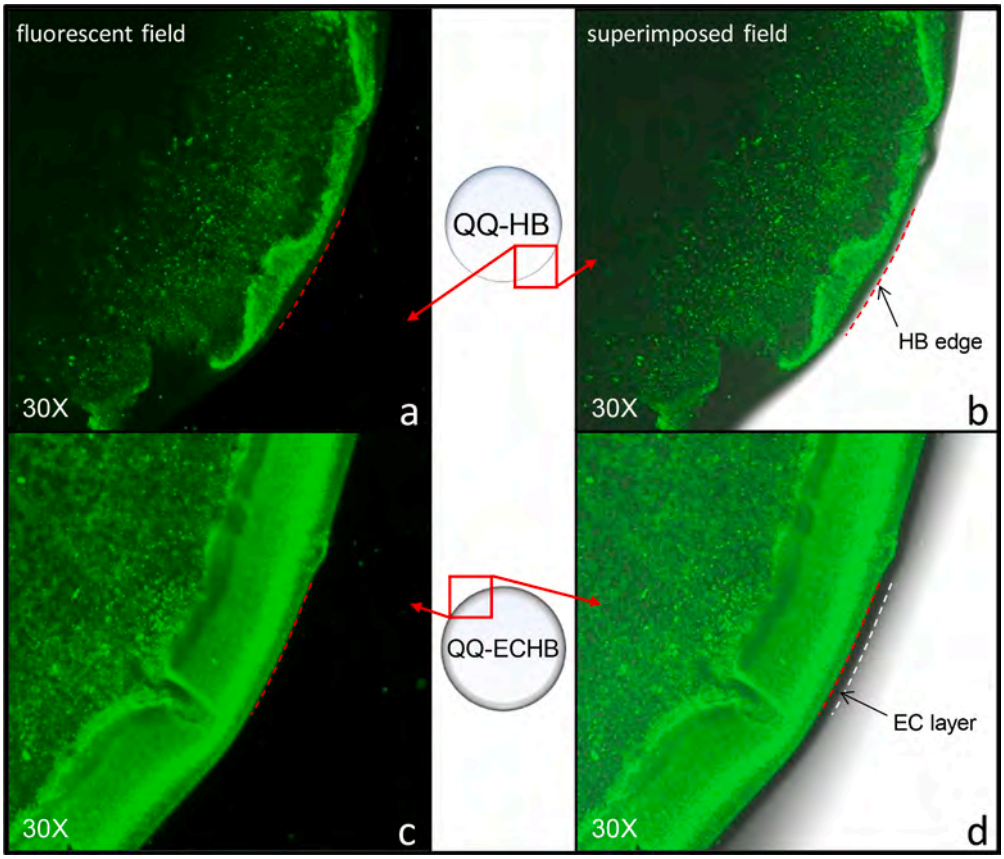

Fig. 3. CLSM images of the cross section of QQ-HB (a, b) and QQ-ECHB (c, d).

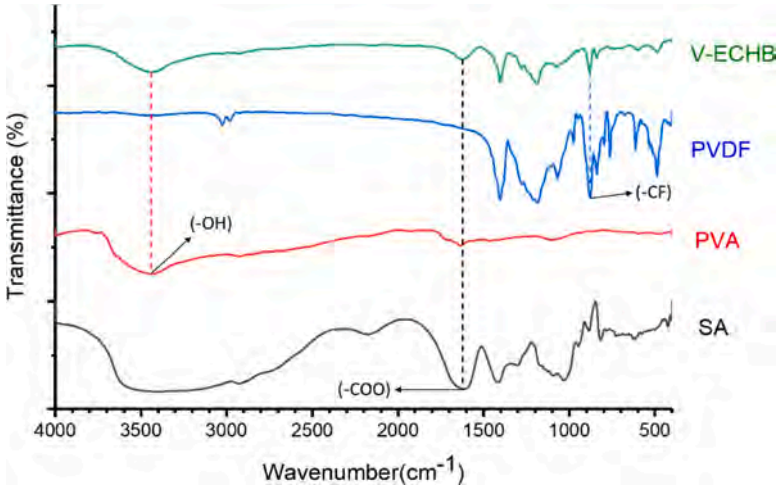

Fig. 4. FT-IR spectra of precursor materials (SA, PVA and PVDF) and freeze-dried V-ECHB.

The pore size distribution of the ES coating was measured using a pore size distribution instrument (POROMETER3G, Quantachrome, USA)(Fang et al. 2014). The membrane sample was cut into a round sample and moistened with the infiltrating fluid, then vacuumed in a sealed environment promotes the discharge of the infiltrating fluid in the membrane pores, software record the pore size distribution through the recorded vacuum pressure-air flow curve and the Washburn formula (eq 1).

$$D = \frac{4\gamma\cos\theta}{p} \quad (1)$$

Where p is the Vacuum pressure, γ is the surface tension of infiltrating liquid, θ is the contact angle.

3. Results and Discussion

3.1. 3D interlayer structure of the QQ-ECHB

To design an advanced multi-layer QQ media applying for mitigate membrane biofouling, the interlayer structure of the QQ-ECHB needs to be investigated. The pristine QQ-HB bead is opaque white, whereas the dehydration treated QQ-HB(g) is translucent yellow. For QQ-ECHB, after being coated with a PVDF porous membrane by electrospinning, the surface coating of the bead reflects a dense white coating (Fig. 2a), and exhibits soft but robust after be stripped away from the hydrogel core (Fig. S2). The surface and internal structures of the beads were characterized via SEM using the freeze-dried samples. Core of the bead with three different stage of treatment shows porous gel crosslinking structure with some wrinkles (Fig. 2b). For the surface layer of the QQ-ECHB, a dense layer with a thickness of 5μm can be observed by SEM under the cross section (Fig. 2c). When the surface layer is biofouling continued to observed at a vertical lens, a 3D porous network covering the whole surface of the hydrogel sphere is revealed (Fig. 2d-g). As the scanning magnification increases, the stacked layered structure assembled of 100nm in diameter nanofiber was observed. From the analysis of the pore diameter distribution of the 3D stacked layer, it is found that the average pore diameter of this layer is 270nm (Fig. S3). This pore size can effectively inhibit the leakage of BH4 bacteria (1-5μm)(Kim et al. 2013) immobilized in the core and continuously keep quorum quenching activity in the MBR, furthermore ensuring that the membrane pore provides a channel unobstructed for soluble ion (0.1nm−1nm) and macromolecular organic matter (2nm-30nm) transfer(2005, Guzenko et al. 2017). In addition, there was no chaotic beads generated in the process of electrospinning, which reinforce the uniformity and continuity of the fiber structure.

3.2. Cell Viability and Distribution of the QQ Media

To investigate the viability of BH4 cell during electrospinning coating, CLSM images of freshly prepared QQ-HB and QQ-ECHB were taken after viability staining. In both type of QQ-media, the bright green fluorescent area of BH4 appeared densely packed and evenly dispersed in the microstructure of the beads and indicates that the QQ bacteria within the beads still maintain their cellular activity after electrospinning process. In order to analyze the distribution of the BH4 cell at inner and surface of the bead in detail, we compared the fluorescence distribution at different locations in the sample section (Fig. 3). By analyzing the QQ-HB slice in fluorescent field and superimposed field, we found that the active bacteria distributed uniformly from the edge of the hydrogel bead to the inner (Fig. 3a-b), comparing with the QQ-ECHB in superimposed field, the edge of the hydrogel is uniformly covered with a 5μm non-fluorescent layer, and we called it electrospinning coating layer (EC layer). To confirm the EC layer is independent of the hydrogel outer layer and without active BH4 cells, the comparison of QQ-ECHB in fluorescent field and superimposed field was introduced, the marked EC layer in Fig. 3d was not developed a fluorescent in Fig. 3c, and a heterogeneous aqueous retaining layer caused by glycerol was visualized between the EC layer and core of the beads.

The above SEM (Fig. 2) and CLSM (Fig. 3) images indicated that a framework of 3D porous nanofiber membrane is successfully assembled on the outer layer of quorum quenching hydrogel beads (QQ-HB) by electrospinning. Physical pore diameter distribution and biological culture test (Fig. S4) were used to verify the ability of the membrane to inhibit the microbial leakage. The proliferation of the colony of different media proved that the robust electrospun coating shell can effectively inhibit the leakage of inner core QQ bacteria compared to QQ-HB. The results verified that the beads with coating reinforcement gained robust physical stability and environmental-tolerance under harsh environmental conditions.

3.3. Chemical Composition Verification of the Carrier

Investigation by FTIR was performed to prove the synthesis of SA, PVA and PVDF in cell carrier (V-ECHB). The infrared spectrum of the precursor materials were measured to grasp its characteristic peaks, comparing to the infrared spectrum of the freeze-dried V-ECHB (Fig. 4).

As for SA, the broad band at 3600–2800 cm^{-1} is linked to the stretching vibrations of OH groups, and the small peaks at 2920–2850 cm^{-1} reflects the CH stretching of aliphatic groups. The band at 1600 cm^{-1} can be ascribed to v(COO) asymmetric vibrations, while the band at 1418 cm^{-1} to v(COO) symmetric vibrations, which is the unique peak

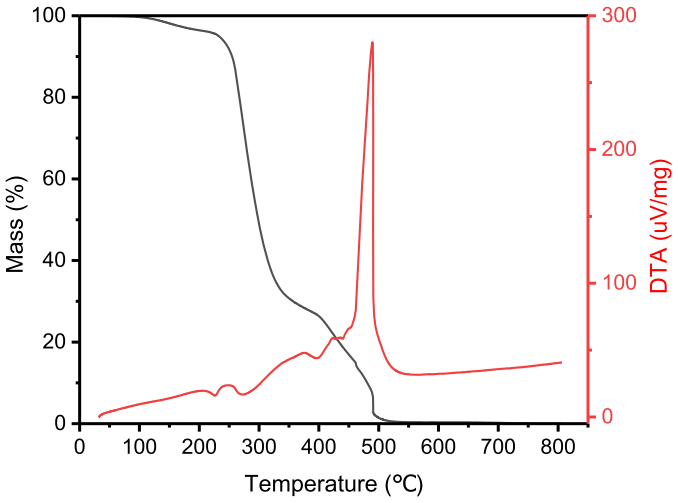

Fig. 5. TGA and DTA thermograms of V-ECHB.

of SA compared with other materials. As could be seen in Fig. 4, the absorption peak of neat PVA at 3290 cm^{-1} were attributed to the asymmetric stretching vibration of OH bond, which is also the only unique peak as compared with V-ECHB. The unique peak of PVDF at 841 cm^{-1}, which is the stretching vibration of CF bond. In summary, the unique spectrum in the precursor materials are all reflected in the infrared spectrum of V-ECHB, indicating that all the precursors are involved in the construction of the chemical structure of V-ECHB.

The TGA and DTA thermograms are present in Fig. 5, the weight loss in the first degradation stage from 100°C to 248°C can be attributed to the loss of diverse volatile compounds like free and bonded water. The endothermic peak of the DTA curve at 248°C reflects the weight change of TGA curve begin to go in another stage from 248°C to 400°C, a 70% dramatic mass decline, which is ascribed to SA-PVA decrosslinking of the polymer network, the formation of carbonaceous fractions and salts. The melting and weight loss of remaining PVDF is confined to a single-step degradation pattern around 450°C, until the V-ECHB is completely degraded around 525°C. The TGA and DTA information of freeze-dried samples proved that the three precursor materials were successfully combined in QQ carrier (V-ECHB).

3.4. Tough 3D Core-Shell Framework Enables Robust Physical Stability and Environmental-Tolerance

We used compression testing to characterize the mechanical robustness of the hydrogel-bacteria beads (radius of 3-4 mm) with varying shell layers (Fig. 6a). We found that beads with an exposed hydrogel core could sustain almost 100% compressive strains and forces up to 13N until the failure of structure, including QQ-HB and V-HB. We

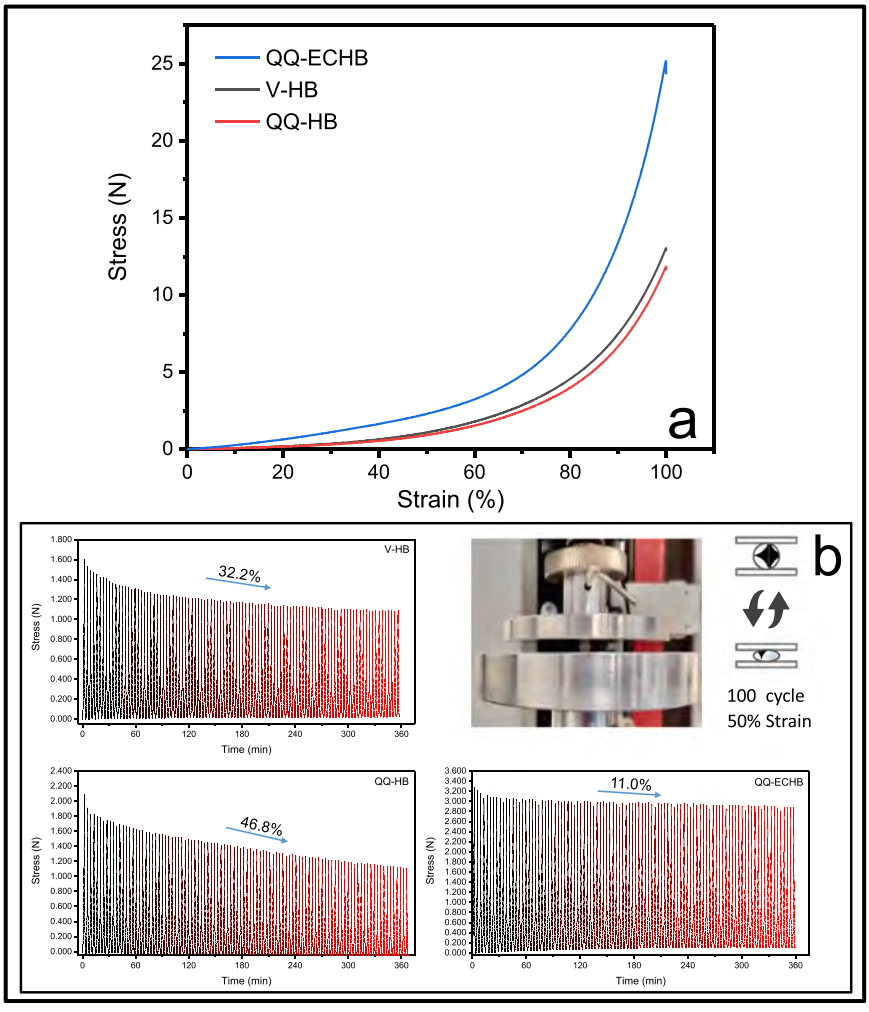

Fig. 6. Stress–strain curves(a) and cyclic compression curves(b) of different media.

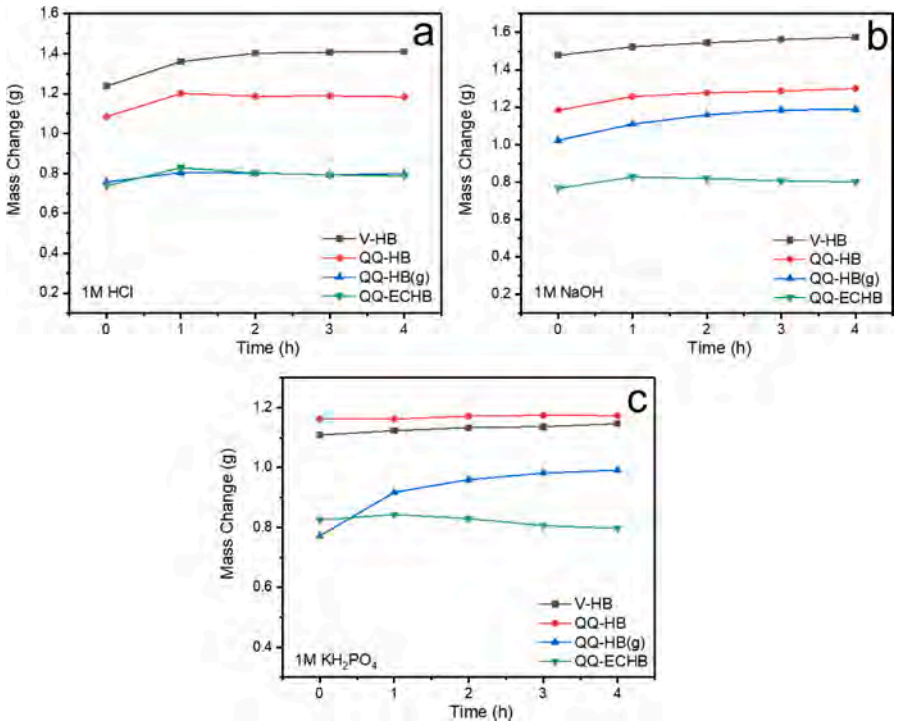

Fig. 7. Mass change of different beads (V-HB, QQ-HB, QQ-HB(g), QQ-ECHB) in HCl (a), NaOH (b) and KH_2PO_4 (C).

further improved the mechanical properties of the beads by fabricating a 3D nanofiber framework layer via electrospinning. With beads that were coated with layer of tough PVDF electrospun coating (QQ-ECHB), we observe the bead is hard to compress and could sustain forces raise to 25N until 100% compressive strains, which is equivalent to subjected to roughly twice the compressive stress of QQ-HB was suffered. The bead capsules were also subjected to cyclic compression at 50% strain (Fig. 6b). With the 100 times cyclic compress within 6h, QQ-ECHB sample shows only 11% reduction of strength. In contrast, the samples with exposed hydrogel core (QQ-HB and V-HB) revealing a 46.8% and 32.2% reduction due to plastic deformation and energy dissipation.

We demonstrated the environmental-tolerance of robust electrospun coating by placing 20 beads in 100mL nonpermissive liquid media and then measure the mass change of beads in stage (Fig. 7). The HCl, NaOH and KH_2PO_4 solutions with the concentration of 1M were selected as the test environment, respectively represent excessive acid, base and salt impact. The results showed that mass change due to the swelling might be a potential challenge in the preliminary stage (0-1h), but could be minimized by the robust electrospun coating. Therefore, a lower rate of mass change of electrospun coating beads could be observed compared with the beads with an exposed hydrogel core. None of one type of beads occurred obvious fragmentation or core disappearance after 4h of exposure.

3.5. *Assessment of the Physical Washing Efficiency of the Carrier*

The QQ-ECHB not only can provide biological QQ activity, because it circulates all the time together with activated sludge under the aeration environment in a MBR for wastewater treatment, but also it may reduce biofouling through collisions and removal of attached biocakes on a membrane surface (physical washing). To examine closely the physical washing contributes to the process of inhibiting membrane fouling, batch experiment under aeration condition was carried out for 3 different types of beads (V-HB, V-ECHB, QQ-ECHB) at the same loading volume of 100mL of the bioreactor volume. The reactors were run for 24h, after which the PVDF coupons were taken out of each reactor and stained with crystal violet.

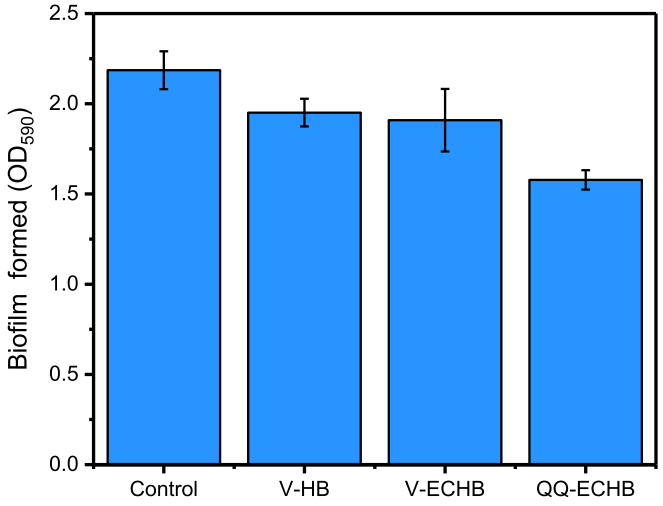

Fig. 8. Comparison of the physical washing effect between V-HB, V-ECHB and QQ-ECHB at the loading volume of 100mL of the bioreactor.

Figure 8 shows the comparison of the physical washing effect between 3 types of beads. The y axis represents the amount of biofilm formed, derived from measuring the concentration of crystal violet, which is proportional to the amount of biofilm attached to a PVDF coupons. The statistical analysis showed that the conventional reactor having no physical washing as a result of a lack of mobile media, had the highest amount of biofilm on the PVDF coupons, whereas the reactor with V-HB had the second highest amount of biofilm and the reactor with V-ECHB had the similar amount of biofilm to V-HB, the reactor with QQ-ECHB had the lowest amount of biofilm. Despite the fact that the vacant beads without QQ activity, but also contributed to the inhibition of membrane biofouling. The result is indicative of a little bit greater cleaning efficiency of V-ECHB than V-HB, possibly as a result of the tougher shell layer of V-ECHB with the bead surface because of their

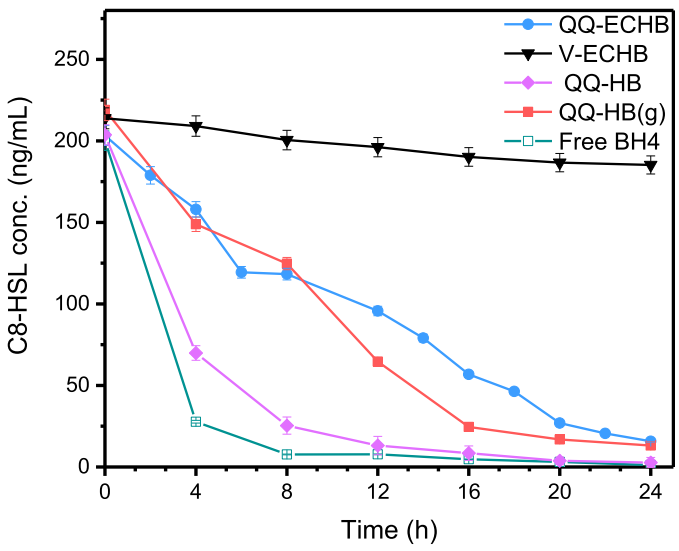

Fig. 9. Quantitative quorum quenching activity of free BH4, V-ECHB, QQ-HB, QQ-HB(g) and QQ-ECHB.

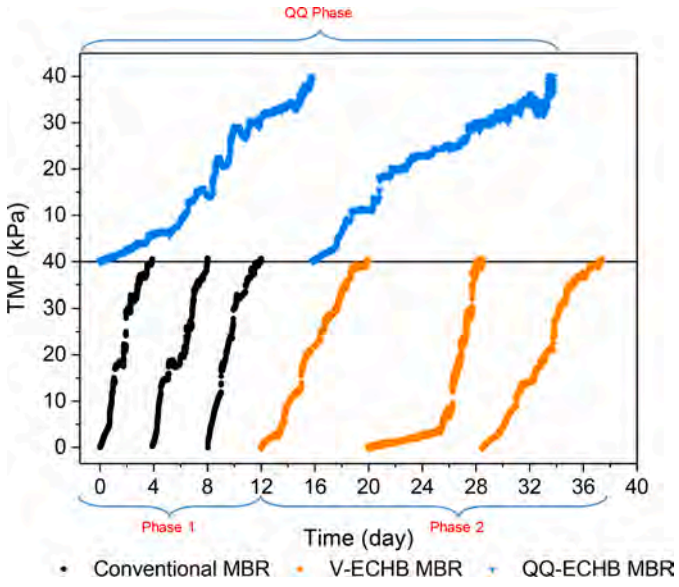

Fig. 10. TMP profiles of conventional MBR, MBR operated with V-ECHB and QQ-ECHB.

robust 3D electrospun coating. In addition, by comparing the difference of the inhibition degree of membrane biofouling between the QQ-ECHB and V-ECHB, it can be estimated that the proportion of physical washing in the overall inhibitory effect was about 38% by dividing the values of the difference between the Control and V-ECHB groups (0.235 OD_{590}) and the difference between the Control and QQ-ECHB groups (0.608 OD_{590}). Therefore, the QQ activity is the key process to inhibit membrane pollution.

3.6. Quorum Quenching Activity of Free BH4 and QQ-Media

The quorum quenching activity of free BH4 and QQ-media was tested using LC-MS with C8-HSL (N-octanoyl-DL-homoserine lactone), which is most abundant in the biofilm-formed membranes in MBR. As shown in Fig. 9, the initial concentration of C8-HSL is 200ng/mL, live BH4 readily degraded C8-HSL to a low concentration within 4h, and was leveled off after 8 hours. QQ-ECHB degraded 87.5% of C8-HSL within 20h, and stabilized at 92.5% in 24h, whereas the V-ECHB removed less than 8% of the C8-HSL in 24h. The comparison verified that quorum quenching bacteria played a major role in degradation of AHL, and the removal by V-ECHB was attributed to its physicochemical adsorption because vacant beads have neither quorum quenching bacteria nor quorum quenching enzyme. By comparing the QQ activity of QQ-ECHB and QQ-HB(g), we found that the QQ-ECHB with an electrospun 3D coating would lead to a pronounced quorum quenching hysteresis due to the sustained release effect of the robust porous shell on mass transfer in the early stage. The swelling of the beads and the activation of the quorum quenching bacteria would postpone to a period of time, it also provides a buffer for the quorum quenching bacteria to adapt to the sewage environment. Nutrients transmissibility experiment by glucose adsorption also proved the penetrability and hysteresis of 3D porous coating, the QQ-HB without the robust porous shell will reach the glucose adsorption equilibrium in advance compared with QQ-ECHB (Fig. S5).

3.7. Application of QQ-ECHB to the MBR

To evaluate the ability of QQ-ECHB to inhibit membrane biofouling and prolong membrane cleaning cycles in MBR, TMP rise-up was monitored in reactor A and B with different applied media, and the profiles of such are shown in Fig. 10. The sludge in the two reactors was acclimated to the same state (SVI: 85~90mL/g) and operated in conventional mode for two weeks before starting record the regulation operations. Reactor A was operated with the addition of QQ-ECHB at a dosage of 10g beads/5L MBR and the TMP rise-up was monitored. Reactor B was operated in conventional mode for 3 periods in the first phase, meaning no media was added. In the second phase of the rector B, V-ECHB were added for 3 periods, to verify the contribution of physical washing on the inhibition of membrane biofouling, every single period ends when the TMP reaching 40kPa, regarded the membrane was completely fouled.

The reactor A in the first period with the addition of QQ-ECHB was operated for 16 days to reach the ending TMP. After cleaned the membrane module, the second period of reactor A also maintained 18 days until completely fouled, compared to the membrane module of conventional mode in reactor A phase 1 was just in an average of 4 days to reach completely fouled in every period. The comparison indicated that the QQ-ECHB can effectively extended the MBR service life nearly 4 times, which verifies the strong mitigation ability of QQ-ECHB on MBR biofouling. In reactor B phase 2, V-ECHB were added, and extended the time for membrane completely fouled to 8 days, which was attributed to the physical washing by the vacant beads. The days of completely fouled for V-ECHB and QQ-ECHB were 8 days and 16 days, respectively, because the number of beads added in both reactors was the same and, hence, it could be assumed that the physical washing effect in the two reactors was the same, the difference biofouling process is likely attributable to the greater QQ activity of QQ-ECHB than of V-ECHB. In

Table 1
Operating conditions and average number of days to reach ending TMP.

Materials	Working Volume (L)	SVI (mL/g)	MLSS (mg/L)	Feed COD (mg/L)	COD removal efficiency (%)	Days to reach TMP 40kPa	Materials state
QQ-HB	5	93	7396	400-500	≧95	12.3(avg)	partial rupture
QQ-ECHB	5	85	6728	360-450	≧95	17.3(avg)	complete & robust
V-ECHB	5	87	6797	360-450	≧95	8.5(avg)	complete & robust

further comparison with data of previous studies (Table 1), QQ-ECHB performs longer days to reach the ending TMP than QQ-HB, and the beads covered with the EC layer retain their structure complete and robust at the end of a MBR cycle, due to the EC layer to inhibit bacteria leakage and to protect the hydrogel core from environmental impact, we also demonstrated this view by comparing the fluorescence intensity of CLSM of the two materials (Fig. S8), QQ-ECHB had higher bacteria count and cell viability than QQ-HB after use.

When the MBR was stopped, the protein (PN) and polysaccharide (PS) of soluble microbial products (SMP) and extracellular polymers (EPS) in activated sludge were measured. PN and PS in EPS and SMP concentrations in both QQ-ECHB MBR were always lower than those in V-ECHB MBR and control MBR. For SMP, loosely bound EPS (LB-EPS) and tightly bound EPS (TB-EPS), the mean concentration in QQ-ECHB MBR at different periods were 10%, 4.5% and 25% lower than in V-ECHB MBR, and 29%, 11% and 32% lower than in vacant MBR, meanwhile the change of protein make up the bulk (Fig. S6). The improvement in EPS and SMP reduction led to enhanced biofouling control in the MBR with QQ-ECHB.

In summary, the MBR with QQ-ECHB was approximately 4 times less prone to membrane fouling compared to the conventional MBR that without media. The 3D core-shell framework of the QQ-ECHB enhances the overall physical strength and protects the durable activity of the quorum quenching bacteria (Fig. S7). The QQ activity of QQ-ECHB is characterized by slow initiation and long duration, it was activated for 3 days and maintained at least 95% QQ activity for 16 days over a MBR cycle, and one of another notable features of QQ-ECHB is the ability to continue to mitigate membrane biofouling in MBR even at very low dosage levels.

4. Conclusions

In this research, by comparing to other studies, QQ-ECHB were more efficient in dosing due to its ability to maintain stable QQ bacteria activity and provide long-lasting quorum quenching effects, these factors contribute to its satisfactory overall performance. The electrospun nanofiber coating of the hydrogel beads with excellent encapsulation and mass transfer performance, this is a breakthrough in our research on the enhancing of hydrogel materials for water treatment, which not only provides a more robust and stable carrier for mitigating the MBR membrane biofouling of the external media, but also provides inspiration for the application of advanced hydrogel materials in other fields like tissue engineering, food engineering and chemical Industry. Electrospinning is a widely adopted additive manufacturing and processing solution. With the emerging of large-scale production lines, there has been a growing trend towards using this technology to produce high-performance materials in bulk. This research represents a significant step in exploring the industrial production of membrane biofouling inhibitors. We have used an automated hydrogel preparation device and a self-developed electrospinning receiver, both of which have significant potential for scale-up. In the future, we aim to increase the material yield while functionalizing the membrane layer and microorganism, enhance quorum quenching with more optimized and efficient material synthesis routes which will allow us to provide biofouling mitigation for larger-scale and unique water quality reactors.

Declaration of competing interest

The authors declare that they have no known competing financial interests or personal relationships that could have appeared to influence the work reported in this paper.

Data availability

Data will be made available on request.

Acknowledgments

This study was supported by the Innovative Province Construction Special Fund of Hunan Province (2020SK2016), the Research Project of Education Department of Hunan Province of China (22A0593), National Natural Science Foundation of China (52000012) and Natural Science Foundation of Hunan Province (2021JJ40578). We especially thank Professor Chung-Hak Lee of the school of Chemical and Biological Engineering, Seoul National University, Republic of Korea for supplying *Rhodococcus* sp. BH4.

Supplementary materials

Supplementary material associated with this article can be found, in the online version, at doi:10.1016/j.watres.2023.119830.

References

Bagheri, M., Mirbagheri, S.A., 2018. Critical review of fouling mitigation strategies in membrane bioreactors treating water and wastewater. Bioresour. Technol. 258, 318–334.
Chen, F., Zhou, D., Wang, J., Li, T., Zhou, X., Gan, T., Handschuh-Wang, S., Zhou, X, 2018. Rational fabrication of anti-freezing, non-drying tough organohydrogels by one-pot solvent displacement. Angew. Chem. Int. Ed Engl. 57 (22), 6568–6571.
Cheng, X., Liu, Y.T., Si, Y., Yu, J., Ding, B., 2022. Direct synthesis of highly stretchable ceramic nanofibrous aerogels via 3D reaction electrospinning. Nat. Commun. 13 (1), 2637.
Diep, E., Schiffman, J.D., 2021. Encapsulating bacteria in alginate-based electrospun nanofibers. Biomater. Sci. 9 (12), 4364–4373.
Drews, A., 2010. Membrane fouling in membrane bioreactors—characterisation, contradictions, cause and cures. J. Membr. Sci. 363 (1-2), 1–28.
Dror, Y., Salalha, W., Avrahami, R., Zussman, E., Yarin, A.L., Dersch, R., Greiner, A., Wendorff, J.H., 2007. One-step production of polymeric microtubes by co-electrospinning. Small 3 (6), 1064–1073.
Ergön-Can, T., Köse-Mutlu, B., Koyuncu, İ., Lee, C.-H., 2017. Biofouling control based on bacterial quorum quenching with a new application: rotary microbial carrier frame. J. Membr. Sci. 525, 116–124.
Fang, Y., Bian, L., Bi, Q., Li, Q., Wang, X., 2014. Evaluation of the pore size distribution of a forward osmosis membrane in three different ways. J. Membr. Sci. 454, 390–397.
Gu, Y., Huang, J., Zeng, G., Shi, L., Shi, Y., Yi, K., 2018a. Fate of pharmaceuticals during membrane bioreactor treatment: Status and perspectives. Bioresour. Technol. 268, 733–748.
Gu, Y., Huang, J., Zeng, G., Shi, Y., Hu, Y., Tang, B., Zhou, J., Xu, W., Shi, L., 2018b. Quorum quenching activity of indigenous quorum quenching bacteria and its potential application in mitigation of membrane biofouling. J. Chem. Technol. Biotechnol. 93 (5), 1394–1400.
Guzenko, D., Chernyatina, A.A. and Strelkov, S.V. (2017) Fibrous Proteins: Structures and Mechanisms. Parry, D.A.D. and Squire, J.M. (eds.), pp. 151-170, Springer International Publishing, Cham.
Huang, J., Gu, Y., Zeng, G., Yang, Y., Ouyang, Y., Shi, L., Shi, Y., Yi, K., 2019a. Control of indigenous quorum quenching bacteria on membrane biofouling in a short-period MBR. Bioresour. Technol. 283, 261–269.
Huang, J., Yang, Y., Zeng, G., Gu, Y., Shi, Y., Yi, K., Ouyang, Y., Hu, J., Shi, L., 2019b. Membrane layers intensifying quorum quenching alginate cores and its potential for membrane biofouling control. Bioresour. Technol. 279, 195–201.
Huang, J., Yi, K., Zeng, G., Shi, Y., Gu, Y., Shi, L., Yu, H., 2019c. The role of quorum sensing in granular sludge: Impact and future application: a review. Chemosphere 236, 124310.
Huang, J., Zhou, J., Zeng, G., Gu, Y., Hu, Y., Tang, B., Shi, Y., Shi, L., 2018. Biofouling control and sludge properties promotion through quorum quenching in membrane bioreactors at two aeration intensities. Biotechnol. Lett 40 (7), 1067–1075.
Huang, J.J., Tian, Y., Chen, L., Liao, Y., Tian, M., You, X., Wang, R., 2020a. Electrospray-printed three-tiered composite membranes with enhanced mass transfer coefficients for phenol removal in an aqueous-aqueous membrane extractive process. Environ. Sci. Technol. 54 (12), 7611–7618.
Huang, S., Mansouri, J., Le-Clech, P., Leslie, G., Tang, C.Y., Fane, A.G., 2022. A comprehensive review of electrospray technique for membrane development: current status, challenges, and opportunities. J. Membr. Sci. 646.
Huang, S., Zhang, H., Albert Ng, T.C., Xu, B., Shi, X., Ng, H.Y, 2020b. Analysis of N-Acy-L-homoserine lactones (AHLs) in wastewater treatment systems using SPE-LLE with LC-MS/MS. Water Res. 177, 115756.
Jayasinghe, S.N., 2022. Unspooling the history of cell electrospinning. Matter 5 (1), 4–7.
Judd, S., 2008. The status of membrane bioreactor technology. Trends Biotechnol. 26 (2), 109–116.
Kang, G.-d, Cao, Y.-m, 2014. Application and modification of poly(vinylidene fluoride) (PVDF) membranes – a review. J. Membr. Sci. 463, 145–165.
Kim, S.R., Oh, H.S., Jo, S.J., Yeon, K.M., Lee, C.H., Lim, D.J., Lee, C.H., Lee, J.K., 2013. Biofouling control with bead-entrapped quorum quenching bacteria in membrane bioreactors: physical and biological effects. Environ. Sci. Technol. 47 (2), 836–842.

Lan, T., Huang, J., Ouyang, Y., Yi, K., Yu, H., Zhang, W., Zhang, C., Li, S., 2021. QQ-PAC core-shell structured quorum quenching beads for potential membrane antifouling properties. Enzyme Microb. Technol. 148, 109813.
Lee, S., Park, S.K., Kwon, H., Lee, S.H., Lee, K., Nahm, C.H., Jo, S.J., Oh, H.S., Park, P.K., Choo, K.H., Lee, C.H., Yi, T., 2016a. Crossing the border between laboratory and field: bacterial quorum quenching for anti-biofouling strategy in an MBR. Environ. Sci. Technol. 50 (4), 1788–1795.
Lee, S.H., Lee, S., Lee, K., Nahm, C.H., Kwon, H., Oh, H.S., Won, Y.J., Choo, K.H., Lee, C. H., Park, P.K., 2016b. More efficient media design for enhanced biofouling control in a membrane bioreactor: quorum quenching bacteria entrapping hollow cylinder. Environ. Sci. Technol. 50 (16), 8596–8604.
Li, S., Huang, J., Yi, K., Pang, H., Liu, Z., Zhang, W., Zhang, C., Liu, S., Li, J., Liu, C., Shu, W., 2023. Silica reinforced core-shell quorum quenching beads to control biofouling in an MBR. Chem. Eng. J. 460.
Li, X., Chen, W., Qian, Q., Huang, H., Chen, Y., Wang, Z., Chen, Q., Yang, J., Li, J., Mai, Y. W., 2020. Electrospinning-based strategies for battery materials. Adv. Energy Mater. 11 (2).
Liang, Y., Zhao, J., Huang, Q., Hu, P., Xiao, C., 2021. PVDF fiber membrane with ordered porous structure via 3D printing near field electrospinning. J. Membr. Sci. 618.
Liu, F., Hashim, N.A., Liu, Y., Abed, M.R.M., Li, K., 2011. Progress in the production and modification of PVDF membranes. J. Membr. Sci. 375 (1-2), 1–27.
Ma, J., Dai, R., Chen, M., Khan, S.J., Wang, Z., 2018. Applications of membrane bioreactors for water reclamation: Micropollutant removal, mechanisms and perspectives. Bioresour. Technol. 269, 532–543.
Manteca, A., Fernandez, M., Sanchez, J., 2005. A death round affecting a young compartmentalized mycelium precedes aerial mycelium dismantling in confluent surface cultures of Streptomyces antibioticus. Microbiology (Reading) 151 (Pt 11), 3689–3697.
Marx, V., 2014. Stop the microbial chatter. Nature 511 (7510), 493–497.
Meng, F., Chae, S.R., Drews, A., Kraume, M., Shin, H.S., Yang, F., 2009. Recent advances in membrane bioreactors (MBRs): membrane fouling and membrane material. Water Res. 43 (6), 1489–1512.
Miller, M.B., Bassler, B.L., 2001. Quorum sensing in bacteria. Annu. Rev. Microbiol. 55 (1), 165–199.
Min, S., Lee, H., Chae, D., Park, J., Lee, S.H., Oh, H.S., Lee, K., Lee, C.H., Chae, S., Park, P. K., 2022. Innovative biofouling control for membrane bioreactors in cold regions by inducing environmental adaptation in quorum-quenching bacteria. Environ. Sci. Technol. 56 (7), 4396–4403.
Nahm, C.H., Choi, D.-C., Kwon, H., Lee, S., Lee, S.H., Lee, K., Choo, K.-H., Lee, J.-K., Lee, C.-H., Park, P.-K., 2017. Application of quorum quenching bacteria entrapping sheets to enhance biofouling control in a membrane bioreactor with a hollow fiber module. J. Membr. Sci. 526, 264–271.
Oh, H.-S., Lee, C.-H., 2018. Origin and evolution of quorum quenching technology for biofouling control in MBRs for wastewater treatment. J. Membr. Sci. 554, 331–345.
Oh, H.S., Yeon, K.M., Yang, C.S., Kim, S.R., Lee, C.H., Park, S.Y., Han, J.Y., Lee, J.K., 2012. Control of membrane biofouling in MBR for wastewater treatment by quorum quenching bacteria encapsulated in microporous membrane. Environ. Sci. Technol. 46 (9), 4877–4884.
Ouyang, Y., Hu, Y., Huang, J., Gu, Y., Shi, Y., Yi, K., Yang, Y., 2020. Effects of exogenous quorum quenching on microbial community dynamics and biofouling propensity of activated sludge in MBRs. Biochem. Eng. J. 157.
Pang, H., Tian, K., Li, Y., Su, C., Duan, F., Xu, Y., 2021. Super-hydrophobic PTFE hollow fiber membrane fabricated by electrospinning of Pullulan/PTFE emulsion for membrane deamination. Sep. Purif. Technol. 274.
Ramakrishna, S., Fujihara, K., Teo, W.-E., Yong, T., Ma, Z., Ramaseshan, R., 2006. Electrospun nanofibers: solving global issues. Mater. Today 9 (3), 40–50.
Shah, S.S.A., Lee, K., Park, H., Choo, K.-H., 2022. Live membrane filters with immobilized quorum quenching bacterial strains for anti-biofouling. J. Membr. Sci. 641.
Shepa, I., Mudra, E., Dusza, J., 2021. Electrospinning through the prism of time. Mater. Today Chem. 21.
Shi, S., Si, Y., Han, Y., Wu, T., Iqbal, M.I., Fei, B., Li, R.K.Y., Hu, J., Qu, J., 2022. Recent progress in protective membranes fabricated via electrospinning: advanced materials, biomimetic structures, and functional applications. Adv. Mater. 34 (17).
Shi, Y., Huang, J., Zeng, G., Gu, Y., Hu, Y., Tang, B., Zhou, J., Yang, Y., Shi, L., 2017. Evaluation of soluble microbial products (SMP) on membrane fouling in membrane bioreactors (MBRs) at the fractional and overall level: a review. Rev. Environ. Sci. Bio/Technol. 17 (1), 71–85.
Shin, D., Kim, J., Chang, J., 2018. Experimental study on jet impact speed in near-field electrospinning for precise patterning of nanofiber. J. Manuf. Processes 36, 231–237.
Tan, J., Kang, B., Kim, K., Kang, D., Lee, H., Ma, S., Jang, G., Lee, H., Moon, J., 2022. Hydrogel protection strategy to stabilize water-splitting photoelectrodes. Nature Energy 7 (6), 537–547.
Tang, T.C., Tham, E., Liu, X., Yehl, K., Rovner, A.J., Yuk, H., de la Fuente-Nunez, C., Isaacs, F.J., Zhao, X., Lu, T.K., 2021. Hydrogel-based biocontainment of bacteria for continuous sensing and computation. Nat. Chem. Biol. 17 (6), 724–731.
Waters, C.M., Bassler, B.L., 2005. QUORUM SENSING: cell-to-cell communication in bacteria. Annu. Rev. Cell Dev. Biol. 21 (1), 319–346.
Wigginton, N.S., 2009. Cutting off communication. Science 326 (5949), 19, 19.
Won-Suk, C., Sang-Ryoung, K., Hyun-Suk, O., Sang, H.L., Kyung-Min, Y., Chung-Hak, L., 2014. Design of quorum quenching microbial vessel to enhance cell viability for biofouling control in membrane bioreactor. J. Microbiol. Biotechnol. 24 (1), 97–105.
Xue, J., Wu, T., Dai, Y., Xia, Y., 2019. Electrospinning and electrospun nanofibers: methods, materials, and applications. Chem. Rev. 119 (8), 5298–5415.
Yeon, K.-M., Cheong, W.-S., Oh, H.-S., Lee, W.-N., Hwang, B.-K., Lee, C.-H., Beyenal, H., Lewandowski, Z., 2009a. Quorum sensing: a new biofouling control paradigm in a membrane bioreactor for advanced wastewater treatment. Environ. Sci. Technol. 43 (2), 380–385.
Yeon, K.-M., Lee, C.-H., Kim, J., 2009b. Magnetic enzyme carrier for effective biofouling control in the membrane bioreactor based on enzymatic quorum quenching. Environ. Sci. Technol. 43 (19), 7403–7409.
Yi, K., Huang, J., Li, X., Li, S., Pang, H., Liu, Z., Zhang, W., Liu, S., Liu, C., Shu, W., 2022. Long-term impacts of polyethylene terephthalate (PET) microplastics in membrane bioreactor. J. Environ. Manage. 323, 116234.
Yi, K., Ouyang, Y., Huang, J., Pang, H., Liu, C., Shu, W., Ye, C., Guo, J., 2023. Evaluating the effect of aeration rate on quorum quenching membrane bioreactors: Performance of activated sludge, membrane fouling behavior, and the energy consumption analysis. J. Environ. Chem. Eng. 11 (1).
Yu, H., Lee, K., Zhang, X., Choo, K.H., 2019. Core-shell structured quorum quenching beads for more sustainable anti-biofouling in membrane bioreactors. Water Res. 150, 321–329.
Zeng, Z., Tang, B., Xiao, R., Huang, J., Gu, Y., Shi, Y., Hu, Y., Zhou, J., Li, H., Shi, L., Zeng, G., 2018. Quorum quenching bacteria encapsulated in PAC-PVA beads for enhanced membrane antifouling properties. Enzyme Microb. Technol. 117, 72–78.
Zhu, T., Jiang, C., Wang, M., Zhu, C., Zhao, N., Xu, J., 2021. Skin-inspired double-hydrophobic-coating encapsulated hydrogels with enhanced water retention capacity. Adv. Funct. Mater. 31 (27).